ELSEVIER

Journal of Nuclear Materials 313–316 (2003) 393–398

journal of nuclear materials

www.elsevier.com/locate/jnucmat

Numerical simulation of CFC and tungsten target erosion in ITER-FEAT divertor

V. Filatov *

D.V. Efremov Scientific Research, Institute of Electrophysical Apparatus, Scientific Technical Centre 'Sintez', Sovetsky prospect 1, Metallostroy, St. Petersburg, Russia

Abstract

Physical, chemical and thermal surface erosion for water-cooled target armoured by CFC and tungsten is simulated by numerical code ERosion OF Immolated Layer (EROFIL-1). Some calculation results on the CFC and tungsten vertical target (VT) erosion in the ITER-FEAT divertor are presented for various operation modes (normal operations, slow transients, ELMs and disruptions). The main erosion mechanisms of CFC armour are the chemical and sublimation ones. Maximum erosion depth per 3000 cycles during normal operations and slow transients is of 2.7 mm at H phase and of 13.5 mm at DT phase. An evaluation of VT tungsten armour erosion per 3000 cycles of H and DT operations shows that no physical or chemical erosion as well as no melting are expected for tungsten armour at normal operations and slow transients. The tungsten armour melting at 2×10^6 ELMs is not allowable. The 300 disruptions are not dangerous in view of evaporation.

PACS: 28.52.Av; 52.40.Hf
Keywords: Erosion; Plasma-facing surface; CFC and tungsten armour; ITER divertor target

1. Introduction

There is a considerable problem with an erosion of tungsten and CFC armour on plasma-facing surface (PFS) in ITER divertor region [1]. This erosion is mainly due to physical and chemical sputtering as well as due to surface heating, sublimation and evaporation under high heat and particle flux at off-normal operation (for example, during plasma transient events). The erosion rate defines the lifetime of the main structural divertor design components on the PFS that is why a numerical simulation of this effect is very important for a design development of plasma-facing components (PFC) especially of vertical target (VT). There are various models as well as the 2D and 3D numerical codes for this purpose, for example [2–5]. But these codes are usually rather complicate because of included models of near-surface plasma and they describe often only partial erosion mechanisms. It is difficult to simulate by these codes a surface erosion evolution during long operation period at the conditions of varying values of heat loads, conductivity of irradiated materials, armour thickness, heat transfer factors, etc. Therefore additional simplified numerical code is very useful to combine the known partial erosion models and to calculate parametrically the maximum possible depth of the PFS erosion (without re-deposition) at factual operation conditions during tokamak divertor lifetime.

2. Erosion model and numerical code

The 1D numerical code ERosion OF Immolated Layer (EROFIL-1) for a simulation of surface complex erosion of water-cooled armour structure is developed. Complete model of erosion includes partial models

* Tel.: +7-812 462 7872; fax: +7-812 464 4623.
E-mail address: filatovv@niiefa.spb.su (V. Filatov).

0022-3115/03/$ - see front matter
PII: S0022-3115(02)01385-5

of physical [6–8], chemical [9,10], radiation-enhanced [11,12] and thermal erosion [13,14] as well as heat transfer model for normal and off-normal operations. Shielding effect on PFS is expected to be calculated by other plasma-physical codes [15] but this effect is still taken into account based on experimental data. Evaporation, heat emission and conduction, water convection, nuclear heating and material irradiation effects are taken into account in the complete model. The code has been verified by testing calculations and comparison with other calculated and experimental data [10,16,17]. It has been found that an agreement is rather good.

3. Operation conditions and calculation assumptions

The operation conditions of the ITER-FEAT divertor and calculation assumptions in various operation modes (normal operation, slow transients, ELMs and disruptions) are presented in Table 1 for H and DT operation phases [18]. Due to vapour shielding effect the disruption deposited energy W_{dis} is less than the incident one W_{dis_in} and depends on disruption duration τ. At the ITER-FEAT conditions it can be estimated by the following formula [19]:

$$W_{dis}\ (\mathrm{MJ/m^2}) = W_{dis\_in}\begin{cases} 10\sqrt{\tau(s)} & \text{for tungsten,} \\ 5\sqrt{\tau(s)} & \text{for CFC.} \end{cases}$$

4. Results of CFC armour erosion evaluation

4.1. Normal operations and slow transients

The results of VT CFC armour erosion evaluation per 3000 cycles of H and DT operations (see Figs. 1–3) are obtained with an account of armour thickness reduction in time and heat conductivity degradation under CFC irradiation up to 0.04 dpa at the DT phase. The maximum erosion depth at the H phase without ELMs and disruptions is about 2.7 mm and corresponds to heat flux of 5 MW/m^2 and ion flux of about 10^{23} ion/m^2 s. Total erosion depth of CFC surface during normal

Table 1
Operation conditions and calculation assumptions for VT armour erosion evaluation

Operation mode	H		DT
Initial temperature of VT armour, °C		115	
Temperature of water cooling flow, °C		115	
Maximum incident ion flux, $m^{-2}\,s^{-1}$	10^{24}		10^{24}
Incident ion energy on armour surface, eV		8	
Incident neutron flux, $m^{-2}\,s^{-1}$	0		10^{17}
Neutron energy, MeV	–		14.1
Maximum irradiation level of armour, dpa	0		0.04
Thickness of armour, mm			
CFC option		20	
Tungsten option		10	
Vacuum pressure nearby armour surface		~0	
Evaporation coefficient		~1	
Normal operations			
Pulse duration, s		400	
Heat load, MW/m^2	5		10
Number of pulses		3000	
Transients			
Duration of transient, s		10	
Heat load, MW/m^2	10		20
Total number of transients		300	
ELMs			
ELM duration, ms		0.1–1	
Energy release density per ELM, MJ/m^2		0.1–1	
Maximum frequency of ELMs, Hz		2	
Disruptions			
Disruption duration, ms		1–10	
Incident energy density per disruption, MJ/m^2	7		10
Total number of disruptions		300	

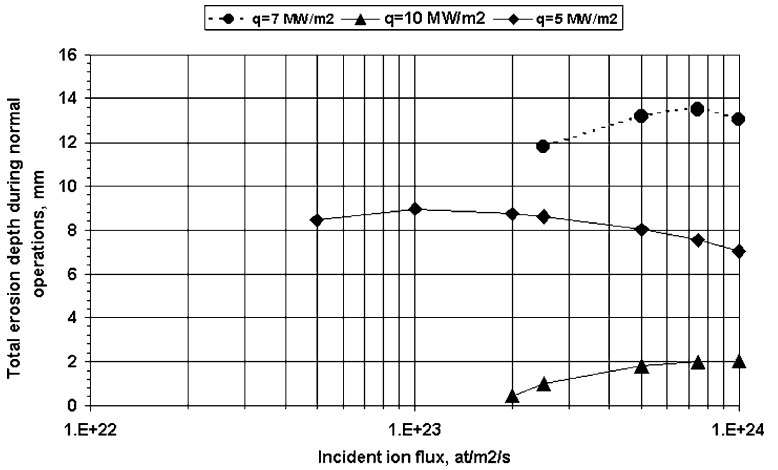

Fig. 1. Total erosion depth of CFC surface during normal DT operations without transients as a function of incident ion flux ($m^{-2}\,s^{-1}$) for various heat loads q.

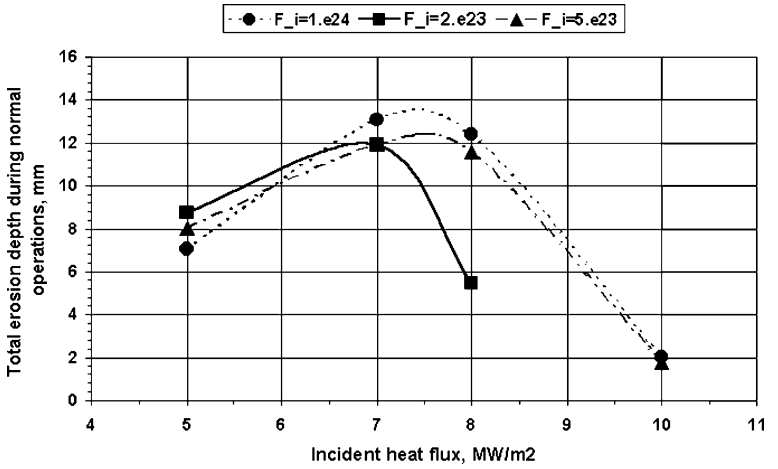

Fig. 2. Total erosion depth of CFC surface during normal DT operations without transients as a function of heat load for various incident ion flux F_i (ion/m^2 s).

DT operations is a function of incident ion flux and heat load. The maximum erosion depth without ELMs and disruptions is about 13.5 mm and corresponds to heat flux of about 7.5 MW/m^2 at normal operations and ion flux of about 10^{24} ion/m^2 s. The slow transients may reduce total erosion as at normal load of 7 MW/m^2 when they reduce total period of operations at temperature of maximum chemical yield. Maximum surface temperature is at the same level during entire operation period, because armour depth reduction is compensated nearly by decrease in heat conductivity under irradiation. The main erosion mechanisms are the chemical and sublimation ones. No physical erosion is expected at incident ion energy of 8 eV in detached plasma mode at the VT area close to strike point. The input of sublimation into total erosion is negligible for normal operations. The fraction of thermal erosion at operations with slow transients is 1.6% (0.2 mm) at normal load of 7 MW/m^2 and 45% (2.1 mm) at 10 MW/m^2 for ion flux of 10^{24} ion/m^2 s. Though maximum surface temperature at slow transients is at the same level of 3000–3200 K for both cases, it is kept for a larger number of pulses for the case of 10 MW/m^2 because of reduced rate of armour thickness reduction by chemical erosion. Total fraction of thermal erosion decreases in time with armour thickness and surface temperature.

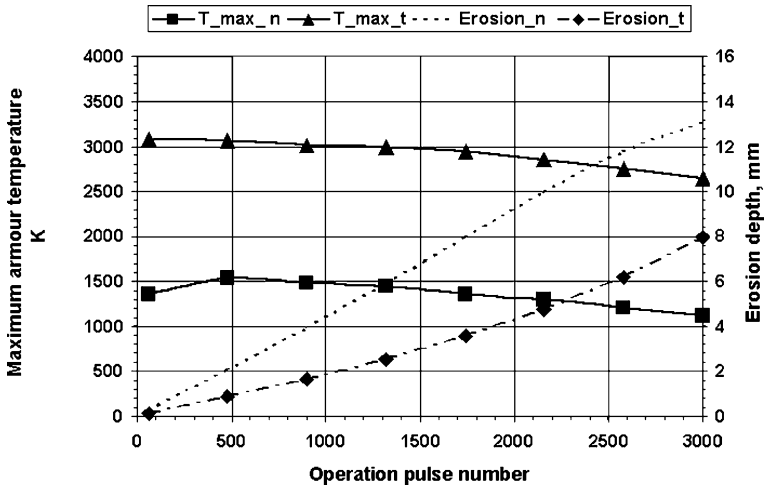

Fig. 3. Time evolution of CFC surface maximum temperature and total erosion depth during DT operations at heat load of 7 MW/m^2 and ion flux of 10^{24} ion/m^2 s without (index '*n*') and with (index '*t*') slow transients (20 MW/m^2).

4.2. ELMs

The ELM events occur periodically during normal operations at thermal plateau. The ELM energy density allowable in view of the CFC armour erosion during the H and DT operations at ELM frequency of 2 Hz is presented in Fig. 4 as a function of the ELM duration. The chemical erosion is not observed at the ELMs in detached plasma mode if initial temperature of ELMs is rather high and exceeds a temperature of intense chemical erosion. Since the ELM duration is rather short the PFS maximum temperature does not depend on armour thickness directly but depends on normal operation plateau temperature that changes with pulse number because the CFC heat conductivity reduces during irradiation.

4.3. Disruptions

The disruptions occur periodically at the thermal plateau of normal operations and break operation pulse. There is no erosion due to disruption at the H operations since maximum surface temperature is rather low. Since the disruption duration is rather short the PFS maximum temperature does not depend on armour thickness but increases with initial temperature (thermal plateau) which one may rise in time (at slow erosion) due to heat conductivity reduction caused by CFC ir-

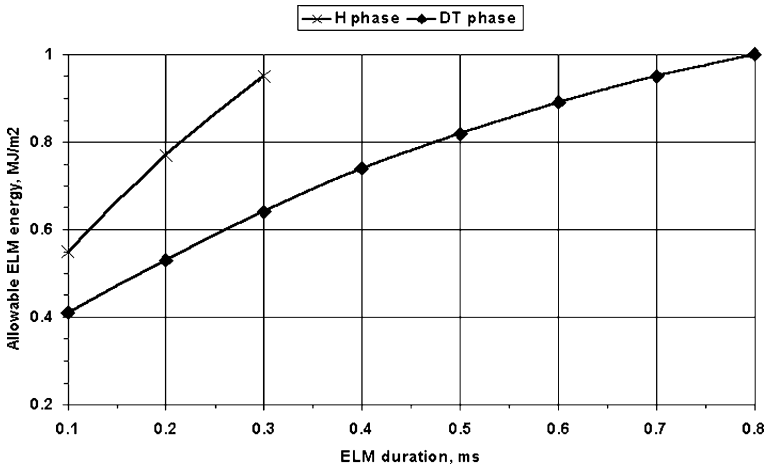

Fig. 4. Allowable ELM energy density in view of the CFC armour erosion during the H and DT operations at ELM frequency of 2 Hz as a function of the ELM duration.

radiation. The calculation for energy density of 10 MJ/m^2 gives total erosion depth of 5.6 mm for disruption duration of 10 ms if no ELM influence is expected (at 0.1 MJ/m^2, 1 ms and 2 Hz). This value includes 2.9 mm of chemical erosion at normal operations, 1.7 mm of sublimation erosion at slow transients and 0.9 mm of sublimation erosion due to all disruptions. A vapour shielding effect is taken into account in a dependence on disruption duration. Thus, an input of disruptions into total erosion depth is allowable at any event duration in the range of 1–10 ms.

5. Results of tungsten armour erosion evaluation

5.1. Normal operations and slow transients

Some results of VT tungsten armour erosion evaluation per 3000 cycles of the H and DT operations are calculated with an account of armour thickness reduction in time. No physical or chemical erosion as well as no melting is expected for tungsten armour at normal operations and slow transients. A sublimation effect is negligible in these modes. The maximum temperature of tungsten/copper joint of 720 °C is obtained in the DT transient mode that seems to be acceptable. The cooling period after a stop of heating does not influence factually on erosion depth for normal operations and increases the erosion by only 3% for each slow transient.

5.2. ELMs

The VT tungsten armour erosion under ELMs is caused both by evaporation and loss of molten layer with droplets. The minimum allowable thickness of tungsten armour is specified by safety reasons as 2 mm therefore for the 10-mm tungsten armour an immolated layer is 8 mm thick. The dependencies of the ELM allowable energy density on the ELM duration calculated for tungsten melting point of 3380 °C are shown in Fig. 5 for ELM frequency of 2 Hz. The maximum surface temperature at the ELMs and disruptions does not depend practically on erosion depth and cooling conditions and depends on initial temperature obtained at thermal plateau of normal operation pulse. The erosion depth is very sensitive to the ELM duration and energy density at the temperature close to melting one. Factually a start of melting causes a very high erosion rate at a fraction of lost molten layer of few percent and above. This can be explained due to very high total number of ELMs (2.4×10^6). That is why the armour melting at ELMs is not allowable if any droplet erosion is expected. If there is no loss of molten layer the erosion is caused only by intensive evaporation of tungsten and allowable energy release density is somewhat higher than for droplet erosion. It is found by the calculations that an allowable depth of tungsten armour erosion at the ELMs suits the following condition for the ELM parameters: $W \leqslant [Q_0 - k\tau]\tau^{0.5}$, where W is deposited energy density (MJ/m^2); τ is event duration (ms). The melting threshold calculated for the ITER VT tungsten armour is constant ($k = 0$) and equal to $Q_0 = 1.54$ for the H operations and $Q_0 = 1.22$ for the DT operations. If droplet erosion of molten material is not expected and melting is acceptable the higher threshold of critical evaporation rate can be described with $Q_0 = 2.4$ and $k = 1.07$ for the H operations as well as with $Q_0 = 2.08$ and $k = 0.8$ for the DT operations.

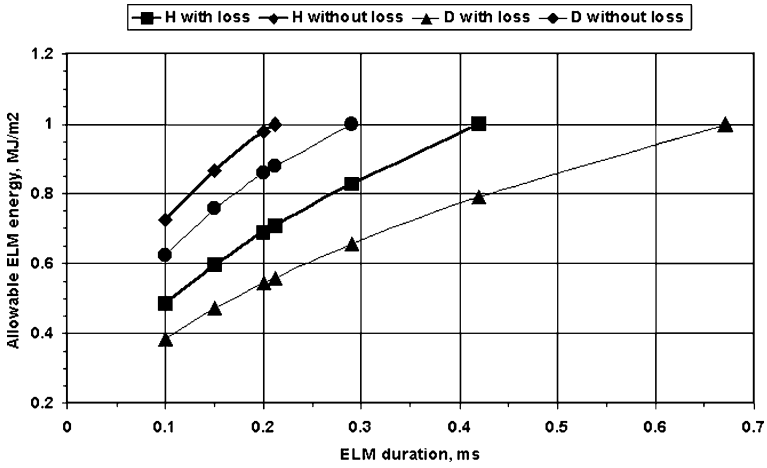

Fig. 5. Allowable ELM energy density in view of tungsten armour erosion during the H and DT operations with and without loss of molten layer at ELM frequency of 2 Hz as a function of the ELM duration.

5.3. Disruptions

The VT tungsten armour erosion under disruptions is caused partly by evaporation but mainly by loss of molten layer. The 300 disruptions are not dangerous without droplet erosion. The 20% loss of molten layer is allowable for any disruption duration in the H-mode but only for short disruptions in the DT-mode when shielding effect is expected. The evaporation component of erosion is rather small, for example, of 0.80 mm (13%) at 1 ms energy release of 10 MJ/m^2.

6. Conclusions

The armour withstands required 3000 operation cycles before divertor cassette replacement in all operation modes except for very short ELMs and long disruptions with maximum possible energy as well as for radiation-enhanced sputtering of CFC at high incident ion fluxes. Physical sputtering erosion is not expected on divertor VT in the mode of 'detached plasma'. The main mechanism of CFC erosion is the chemical one. Tungsten armour is eroded mainly through partial loss of molten layer due droplet splashing at short ELMs and disruptions.

References

[1] G. Federici et al., Nucl. Fusion 41 (R12) (2001) 1967.
[2] A. Hassanein, I.I. Konkashbaev, Fusion Eng. Des. 28 (1995) 27.
[3] I. Smid, H.D. Pacher, G. Vieider, et al., J. Nucl. Mater. 233–237 (1996) 701.
[4] A.R. Raffray, G. Federici, J. Nucl. Mater. 244 (1997) 85.
[5] G. Tsotridis, Fusion Technol. 37 (2000) 185.
[6] J. Bohdansky, Nucl. Instrum. and Meth. B 2 (1984) 587.
[7] W. Eckstein et al., Report IPP 9/82, Max-Planck Institute, Garching, Germany, 1993.
[8] P. Mioduszewski, Fusion Technol. 32 (2) (1997) 277.
[9] J. Roth, J. Nucl. Mater. 266–269 (1999) 51.
[10] D.G. Whyte et al., Nucl. Fusion 41 (1) (2001) 47.
[11] J. Roth, J. Nucl. Mater. 145–147 (1987) 87.
[12] J. Roth, E. Vietzke, A.A. Haasz, Nucl. Fusion Suppl. 1 (1991) 63.
[13] L.N. Topilsky, VANT: Fusion (1) (1982) 33 (in Russian).
[14] R. Behrisch, J. Nucl. Mater. 93&94 (1980) 498.
[15] H. Wuerz, I. Landman, B. Bazylev, et al., J. Nucl. Mater. 233–237 (1996) 798.
[16] C. Garsia-Rosales, J. Roth, J. Nucl. Mater. 196–198 (1992) 573.
[17] G. Federici, A.R. Raffray, J. Nucl. Mater. 244 (1997) 101.
[18] G. Federici et al., J. Nucl. Mater. 290–293 (2001) 260.
[19] A.M. Zhitlukhin, private communication, June 2001.